NEUROPATHOLOGY

Neuropathology 2020; **40**, 570–586 doi:10.1111/neup.12694

Original Article

Praja1 RING-finger E3 ubiquitin ligase suppresses neuronal cytoplasmic TDP-43 aggregate formation

Kazuhiko Watabe,[1,2] Yoichiro Kato,[2] Miho Sakuma,[3] Makiko Murata,[1] Motoko Niida-Kawaguchi,[2] Taro Takemura,[4] Nobutaka Hanagata,[4] Mari Tada,[5] Akiyoshi Kakita[5] and Noriyuki Shibata[2]

[1]Department of Medical Technology (Neuropathology), Kyorin University, [2]Department of Pathology, [3]School of Medicine, Tokyo Women's Medical University, Tokyo, [4]Research Network and Facility Services Division, National Institute for Materials Science, Tsukuba and [5]Department of Pathology, Brain Research Institute, Niigata University, Niigata, Japan

Transactivation response DNA-binding protein of 43 kDa (TDP-43) is a major constituent of cytoplasmic aggregates in neuronal and glial cells in cases of amyotrophic lateral sclerosis (ALS) and frontotemporal lobar degeneration (FTLD). We have previously shown neuronal cytoplasmic aggregate formation induced by recombinant adenoviruses expressing human wild-type and C-terminal fragment (CTF) TDP-43 under the condition of proteasome inhibition *in vitro* and *in vivo*. In the present study, we demonstrated that the formation of the adenoviral TDP-43 aggregates was markedly suppressed in rat neural stem cell-derived neuronal cells by co-infection of an adenovirus expressing heat shock transcription factor 1 (HSF1), a master regulator of heat shock response. We performed DNA microarray analysis and searched several candidate molecules, located downstream of HSF1, which counteract TDP-43 aggregate formation. Among these, we identified Praja 1 RING-finger E3 ubiquitin ligase (PJA1) as a suppressor of phosphorylation and aggregate formation of TDP-43. Co-immunoprecipitation assay revealed that PJA1 binds to CTF TDP-43 and the E2-conjugating enzyme UBE2E3. PJA1 also suppressed formation of cytoplasmic phosphorylated TDP-43 aggregates in mouse facial motor neurons *in vivo*. Furthermore, phosphorylated TDP-43 aggregates were detected in PJA1-immunoreactive human ALS motor neurons. These results indicate that PJA1 is one of the principal E3 ubiquitin ligases for TDP-43 to counteract its aggregation propensity and could be a potential therapeutic target for ALS and FTLD.

Key words: adenovirus, amyotrophic lateral sclerosis, frontotemporal lobar degeneration, Praja1, TDP-43.

INTRODUCTION

Formation of neuronal and glial cytoplasmic aggregates containing transactivation response DNA-binding protein of 43 kDa (TDP-43), a DNA/RNA-binding protein that localizes predominantly to the nucleus and shuttles between the cytoplasm and nucleus, is one of the pathological hallmarks of amyotrophic lateral sclerosis (ALS) or frontotemporal lobar degeneration with TDP-43-positive inclusions (FTLD-TDP).[1–5] In pathological situations, full-length wild-type (WT) TDP-43 is cleaved to form a 25-kDa C-terminal fragment of TDP-43 (CTF TDP-43) lacking nuclear localization signal (NLS) that is localized to the cytoplasm. The C-terminal region of TDP-43 contains a prion-like domain that have aggregation-prone properties. Cytoplasmic TDP-43 aggregates are phosphorylated, ubiquitinated, and likely composed of WT and CTF TDP-43.[1–5] The formation of cytoplasmic TDP-43 aggregates has been attributed to multiple factors, including impaired RNA and/or protein metabolism, stress granule formation, and oxidative stress.[6] Among these, impairment of proteolytic machineries, including proteasome, endosome and autophagy systems, has been shown to play a key role in TDP-43 aggregate formation.[1,7] We have previously shown that proteasome inhibition enhanced the formation of adenovirally expressed TDP-43 cytoplasmic aggregates both *in vitro* and *in vivo*, suggesting that impairment of protein degradation

Correspondence: Kazuhiko Watabe, MD, PhD, Department of Medical Technology (Neuropathology), Kyorin University Faculty of Health Sciences, 5-4-1 Shimorenjaku, Mitaka, Tokyo 181-8612, Japan. Email: watabe@ks.kyorin-u.ac.jp

Received 27 April 2020; revised 22 May 2020; accepted 25 May 2020; published online 19 July 2020.

pathways accelerates the formation of TDP-43-positive aggregates.[8] *In vitro* time-lapse imaging analyses revealed growing cytoplasmic aggregates in the TDP-43 adenovirus-infected neuronal and glial cells, followed by collapse of the cells. These TDP-43 aggregates remained insoluble in culture media, consisted of sarkosyl-insoluble granular materials, and contained phosphorylated TDP-43.[9] The released aggregates were incorporated into neighboring neuronal cells, indicating cell-to-cell spreading[9] that is in line with the prion-like propagation hypothesis that explains progression of neurodegenerative diseases such as prion disease, Alzheimer's disease, Huntington's disease, and Parkinson's disease, as well as ALS/FTLD.[10–12]

Recently, several reports have demonstrated that heat shock transcription factor 1 (HSF1),[13,14] a master regulator of heat shock response, and its downstream heat shock proteins, including heat shock protein 70 (HSP70),[15] HSPB8,[16–19] HSP40/DNAJB2a,[20] HSP40/DNAJB1, HSP27[21] and clusterin,[22] mediate clearance of aggregated TDP-43 species.

In the present study, we demonstrate that the formation of the adenoviral TDP-43 aggregates was markedly suppressed by co-infection of an adenovirus expressing HSF1. DNA microarray analysis was performed to identify candidate molecules located downstream of HSF1 that counteract TDP-43 aggregate formation. Among these, we identified Praja 1 RING-finger E3 ubiquitin ligase (PJA1) as a suppressor of phosphorylation and aggregate formation of TDP-43.

MATERIALS AND METHODS

Adult rat neural stem cell line 1464R

All experiments were performed in accordance with Japanese National Guidelines and Regulations, and were approved by the Biosafety Committee and the Animal Care and Use Committee of the Kyorin University Faculty of Health Sciences. The 1464R adult rat neural stem cell line was established as previously described[8,9,23] (#T0746; Applied Biological Materials, Richmond, Canada) and cells were cultured in growth medium composed of Neurobasal medium (#21103-049; Thermo Fisher Scientific, Waltham, CA, USA) containing 2 mM L-glutamine (#25030-081; Thermo Fisher), 2% B27 supplement (#17504-044; Thermo Fisher), 10 ng/mL fibroblast growth factor 2 (FGF2) (#F0291; Sigma, St. Louis, MO, USA), 10 ng/mL epidermal growth factor (EGF) (#E9644; Sigma), 50 units/mL penicillin and 50 μg/mL streptomycin (#15070-063; Thermo Fisher) on 10-cm dishes coated with poly(2-hydroxyethylmethacrylate) (PHEMA) (#P3932; Sigma) to prevent cell attachment. Cells were maintained in 5% CO_2 at 37°C. The 1464R cells formed typical neurospheres, and were mechanically dissociated, serially passaged in the same medium twice a week, and cultured further for more than 50 passages with no obvious morphological alterations. To differentiate 1464R cells into neuronal and glial cells, dissociated 1464R cells were seeded on poly-L-lysine (PLL) (#P1524; Sigma) -coated 12-well plates or 9-mm ACLAR round coverslips (Allied Fibers & Plastics, Pottsville, PA, USA) at a density of $4–5 \times 10^5$ cells per well and $1–2 \times 10^4$ cells per coverslip, respectively, and maintained in differentiation medium composed of F12 medium (#11765-054; Thermo Fisher) containing 5% fetal bovine serum (Moregate, Australia), 0.5% N2 supplement (#17502-048; Thermo Fisher), 1% B27 supplement, 1 μM all-trans retinoic acid (ATRA) (#R2625; Sigma), 50 units/mL penicillin, and 50 μg/mL streptomycin in 5% CO_2 at 37°C. For transient transfection of plasmids, 1464R cells dissociated and seeded on coverslips in differentiation medium were immediately transfected with plasmids as described below using Fugene 6 Transfection Reagent (#E2691; Promega, Madison, WI, USA) according to the manufacturer's instructions. Two days after, the cells were fixed with 4% paraformaldehyde (PFA) in phosphate buffered saline (PBS) and examined under an Olympus AX80TR microscope equipped with a DP70 CCD camera.

Adenovirus infection

Preparation of recombinant adenovirus vectors encoding DsRed-tagged full-length human WT (AxDsRhWTTDP43; RIKEN DNA Bank Japan; #RDB15499) and CTF (208-414aa of TDP-43) (AxDsRhCTFTDP43; RIKEN #RDB15500) human TDP-43 cDNAs have been previously described.[8,9] Adenovirus vectors encoding DsRed-tagged WT and CTF human TDP-43 containing FLAG tag (5′-CTTGTCATCGTCGTCCTTGTAGTC-3′) at the 3′-ends (AxDsRhWTTDP43FLAG, AxDsRhCTFTDP43FLAG) were newly constructed for co-immunoprecipitation (Co-IP) experiments as described below. For the construction of adenovirus encoding EGFP-tagged WT and dominant negative human HSF1 and candidate genes (Table 1), cDNAs obtained from HEK 293 and 1464R cells by reverse transcription-polymerase chain reaction (RT-PCR) using primers as listed in Table 2 were successively cloned into pEGFPN1-3 (Clontech, Palo Alto, CA, USA) and adenovirus cassette cosmid pAxCAwtit2 (TaKaRa, Osaka, Japan) as described.[8,9] Human UBE2E3 cDNA was cloned into pcDNA3.1MycHis (V80020; Thermo Fisher) and the resulting UBE2E3MycHis fragment was subcloned into pAxCAwtit2. The cosmids were then transfected to 293 cells and recombinant adenovirus vectors were propagated and isolated from 293 cells, and purified using a ViraBind Adenovirus Purification Kit (#VPK-100; Cell Biolabs, San Diego, CA, USA). Neurons and glial cells differentiated from 1464R cells on PLL-coated 6 or 12 well plates or 9-mm coverslips were infected with adenoviruses at a multiplicity of infection

Table 1 Candidate molecules that suppress TDP-43 aggregate formation

Gene	Rat accession number	Description	HSF1/EGFP fold change	
			Vehicle[†]	AxDsRTDP43/MG-132[‡]
Acp5	NM_019144	Acid phosphatase 5, tartrate resistant (tartrate-resistant acid phosphatase; TRAP)	9.0 2.3	45.4 11.2
Amigo2	NM_182816	Adhesion molecule with Ig-like domain 2 (Alivin 1; ALI1)		
Creb3l1	NM_001005562	cAMP responsive element binding protein 3-like 1 (old astrocyte specifically induced substance; OASIS)	2.1	10.1
Pja1	NM_001101006	Praja RING-H2 finger E3 ubiquitin ligase 1	2.8	6.9
Hebp2	NM_001107515	Heme binding protein 2	2.9	5.8
Dnajb2	NM_001109541	DnaJ heat shock protein family (Hsp40) member 2	1.3	1.5

[†]Fold change by HSF1 transduction.

[‡]Fold change in association with inhibition of TDP-43 aggregate formation by HSF1 transduction.

Table 2 PCR primers used in this study

Gene	Primer
Human HSF1	F: ATAAGCTTATATGGATCTGCCCGTGGGCCCCGGCG
(NM_005526)	R: TGGTACCTAGGAGACAGTGGGGTCCTTGGCTTTGG
Human HSF1Δ	F: TCAAGCTTGGGTACCATGGATCTGCCCGTG
(del. 380–529)	R: CAGAATTCTCCAGGCAGGCTACGCTGAGGCACTTT
Rat ACP5	F: GCAAGCTTGCCACCATGACCACCTGTGCTTCCTCCAG
(NM_019144)	R: ATGGATCCAGGGTCTGGGTCGCCTGGGGAGGCTG
Rat AMIGO2	F: ACTCGAGCCACCATGTCGTTAAGGTTCCACACACTG
(NM_182816)	R: TGAATTCAGTGGATGCCACGAAGGGGGTGTCTGA
Rat CREB3L1	F: GCAAGCTTGCCACCATGGACGCCGTCTTGGAACCTT
(NM_001005562)	R: TGAATTCGGAGAGTTTGATGGTGGTGTTGGGGCC
Rat HEBP2	F: ATAAGCTTGCCACCATGGCAGAAGAGCCAGACCTC
(NM_001107515)	R: CGAATTCCTTGTCTTCATCGGAGGGCTCGTTTCTC
Human DNAJB2a	F: AGGGATCCACCATGGCATCCTACTACGAGATCCTA
(NM_001039550)	R: GAGCGGCCGCTCAGAACACATCTGCGGGTTTCTTC
Rat PJA1x4	F: GCAAGCTTGCCACCATGAGCCAGCAGGAGAGGATTGC
(NM_001101006)	R: TGAATTCGAGCGGGGGAGGGAACATGCAGCGGCAC
Rat PJA1x1	F: GCAAGCTTGCCACCATGGGTCAGGGATCTAGCAAGCC
(XM_006257105)	R: TGAATTCGAGCGGGGGAGGGAACATGCAGCGGCAC
Rat PJA1ΔR	F: GCAAGCTTGCCACCATGGGTCAGGGATCTAGCAAGCC
(del. 574–617)	R: TGAATTCCATTTCCTGGCCCACTGCACCGTGATCTTC
Human PJA1v1	F: GCAAGCTTGCCACCATGGGTCAGGAATCTAGCAAGCC
(NM_145119)	R: TGAATTCGAGTGGGGGAGGGAACATGCAGCGGCA
Human PJA1ΔR	F: GCAAGCTTGCCACCATGGGTCAGGAATCTAGCAAGCC
(del. 594–637)	R: CTGAATTCCATCTCCTGACCAACTGCGCCATGATC
Human UBE2E3	F: GTAAGCTTGCCACCATGTCCAGTGATAGGCAAAGG
(NM_006357)	R: GTGGATCCGATGTTGCGTATCTCTTGGTCCACTGT

F, forward; PCR, polymerase chain reaction; R, reverse.

(MOI) of 50. Twenty-four hours later, the cells were refed with the media with or without MG-132 (#474790; Merck Millipore/Calbiochem, Burlington, MA, USA) and further incubated for 24 h. In some experiments, proteasome inhibitors lactacystin (#426100; Calbiochem), epoxomicin (#426100; Calbiochem) and bortezomib (#021-18 901; FUJI FILM Wako, Osaka, Japan) were used instead of MG-132, and the effects of autophagy inhibitors 3-methyladenine (#M9281; Sigma), bafilomycin A1 (#B1793; Sigma) and wortmannin (#W1628; Sigma) were also examined. The treated cells on the dishes or coverslips were lysed for Western blotting or fixed for immunocytochemistry, respectively, as described below. DsRed or EGFP fluorescence in living cells was examined under an Olympus IX70 inverted fluorescence microscope equipped with a DP72 CCD camera prior to cell lysate preparation or fixation.

Cell fractionation, co-immunoprecipitation, and Western blot analysis

For cell fractionation, cultured cells in 12-well plates ($4\text{-}5 \times 10^5$ cells/well) were lysed in 50 μL of

radioimmunoprecipitation assay (RIPA) buffer, consisting of 50 mM Tris–HCl pH 8.0, 150 mM NaCl, 5 mM EDTA, 1% Nonidet P-40, 0.5% sodium deoxycholate, and 0.1% sodium dodecyl sulfate (SDS), supplemented with cOmplete protease inhibitor (#11697498001; Sigma) and PhosSTOP phosphatase inhibitor (#4906845001; Sigma) cocktails, sonicated for 15 s twice, and incubated for 30 min on ice followed by centrifugation at 20 000 *g* for 90 min at 4°C. The supernatants and pellets were collected as RIPA-soluble and insoluble fractions, respectively, lysed in 1× SDS-sample buffer containing 2-mercaptoethanol (ME), and treated for 5 min at 95°C. Protein concentration of each supernatant fraction was determined with a Qubit Protein Assay Kit (Thermo Fisher).

For Co-IP, 1464R cells in 6-well plates (6×10^5 cells/well) were lysed in 200 μL of IP buffer (50 mM Tris–HCl pH 7.4, 150 mM NaCl, 1 mM EDTA, 1% Nonidet P-40, 5% glycerol) containing cOmplete, PhosSTOP inhibitor cocktails and de-ubiquitination inhibitor PR-619 (#16276; Cayman, Ann Arbor, MI, USA), incubated for 30 min on ice followed by centrifugation at 12000 *g* for 30 min at 4°C. Ten percent of the resulting supernatants was analyzed as the input cell lysate, and the remaining 90% of supernatants was incubated with anti-FLAG M2 affinity gel (#A2220; Sigma) for 3 h at room temperature by rotator shaker. The affinity gel was washed three times with Tris buffered saline (TBS) consisting of 50 mM Tris–HCl (pH 7.4) and 150 mM NaCl. The inputs and immunoprecipitates were lysed in 1× SDS-sample buffer containing 2-ME and treated for 5 min at 95°C.

Fractionated cell lysates (10–20 μg) or immunoprecipitates were electrophoresed on 4–20% SDS/polyacrylamide gels under reduced conditions and transferred to PVDF membrane (Atto, Tokyo, Japan). The blotted membrane was blocked with 3% skim milk and incubated overnight with rabbit anti-FLAG (#7425; Sigma), rabbit anti-TDP-43 C-terminus (405-414) (#TIP-TDP09; Cosmo Bio, Tokyo, Japan), rabbit anti-phosphorylated TDP-43 (pSer409/S410) (#TIP-PTD-P02; Cosmo Bio), rabbit anti-PJA1 (#17687-1-AP; ProteinTech Japan, Tokyo, Japan), rabbit anti-Myc Tag (#2278; Cell Signaling Technology, Danvers, MA, USA), rabbit anti-ubiquitin K48 (#05-1307; Sigma), rabbit anti-UBE2D2/3 (#HPA003921: Sigma), rabbit anti-UBE2E3 (#15488-1-AP; ProteinTech), rabbit anti-UBE2K (#11834-3-AP; ProteinTech), and mouse monoclonal anti-GAPDH (#ab8245; Abcam, Cambridge, UK) antibodies at dilutions of 1:1000, followed by incubation with biotinylated anti-rabbit or anti-mouse IgG (Vector Laboratories, Burlingame, CA, USA; 1:1000) for 1 h and streptavidin-alkaline phosphatase (#11089161001; Sigma; 1:1000) for 1 h. Reactions were visualized by color development using nitroblue tetrazolium chloride (NBT) and 5-bromo-4-chloro-3-indolylphosphate p-toluidine salt (BCIP) (#11681451001; Sigma). In some experiments, immunoblotted TDP-43 CTF and GAPDH (as loading control) bands were quantified by ImageJ software (NIH, USA).

Cell viability assay

For cell viability assay, differentiated 1464R cells were seeded on PLL-coated 96-well plates (5×10^4 cells /well) and cultured in differentiation medium. After 4 days, the cells were infected with adenoviruses at an MOI of 50. Twenty-four hours later, the cells were refed with the media with or without 0.5–2 μM MG-132 (Sigma) and further incubated for 24–48 h. The cells were then incubated with cell counting kit-8 (CCK-8) solution (#CK04; DOJINDO, Tokyo, Japan; 10 μL/200 μL culture medium) for 4 h, and the absorbance at 450 nm was measured with a microplate reader.

Immunocytochemistry

Cells were fixed with 4% PFA in PBS, permeabilized with 100% methanol, washed with PBS, and immunostained overnight at 4°C with mouse monoclonal TuJ1 (#MAB1195; R&D systems, Minneapolis, MN, USA) at a dilution of 1:200. The cells were then incubated with Alexa Fluor 350-conjugated goat anti-mouse IgG (Thermo Fisher) at 1:400 dilution for 1 h at room temperature, followed by incubation for 15 min with 2 μg/mL Hoechst 33342 (Thermo Fisher). After washing, coverslips were mounted on glass slides with Gelvatol (20% glycerol/10% polyvinyl alcohol in 0.1 M Tris–HCl pH 8.0). Immunostained cells were examined under the Olympus AX80TR microscope equipped with a DP70 CCD camera.

Animal surgery and histological analysis

The experimental protocols were approved by the Animal Care and Use Committee of the Kyorin University Faculty of Health Sciences. Adult ICR male mice (8–10 weeks old, 40–45 g) were anesthetized with intraperitoneal injection of a combination anesthetic (M/M/B: 0.3/4/5) prepared with 0.3 mg/kg of medetomidine, 4.0 mg/kg of midazolam, and 5.0 mg/kg of butorphanol.[24] Under a dissecting microscope, the right facial nerve was exposed and 6 μL solution in total of recombinant adenoviruses (1×10^8 plaque-forming units [pfu] each for combined injection) was slowly injected into the main trunk (marginal branch) of the facial nerve using a 33G microsyringe (Hamilton, Reno, NV, USA). The virus suspension was mixed with Evans Blue (0.01% final; Sigma) to confirm visually that the injection had been successfully performed.

Four days after operation, mice were anesthetized by inhalation with a lethal dose of isoflurane and transcardially perfused with 0.1 M phosphate buffer, pH 7.4 (PB) followed by 4% PFA in 0.1 M PB. The brain stem tissue containing facial nuclei was dissected,

immersion fixed in the same fixative, and cryoprotected in 30% sucrose in 0.1 M PB. Serial 10-μm-thick transverse sections were made by cryostat. To enhance EGFP detection in PJA1EGFP adenovirus-treated samples, cryostat sections were permeabilized with 100% methanol, washed with PBS, preincubated with 5% normal goat serum (Invitrogen) in PBS, and immunostained overnight at 4°C with rabbit anti-GFP (#ab6556; Abcam) at a dilution of 1:1000, followed by incubation with Alexa 488-conjugated goat anti-rabbit IgG (Invitrogen) at a 1:1000 dilution for 1 h at room temperature. The sections were counterstained with 2 μg/mL Hoechst 33342 (Thermo Fisher), mounted with Gelvatol and examined under the Olympus AX80TR microscope equipped with a DP70 CCD camera. For motor neuron cell counting (n = 4), every fifth section at a thickness of 10 μm was picked up and at least 250 facial motor neurons having Hoechst 33342-counterstained nuclei were counted in five sections, so that these neurons were counted only once in every fifth section with a 40-μm interval.

Immunohistochemistry on human tissue sections

All experiments were approved by and performed under the guidelines of the Kyorin University Ethics Committee, the Tokyo Woman's Medical University Ethics Committee and the Niigata University Ethics Committee. Informed consent was obtained from all individuals or their guardians before the autopsy analysis. Postmortem lumbar spinal cords from five patients definitely diagnosed as having sporadic ALS and from four non-diseased control cases were fixed with 10% buffered formalin and embedded in paraffin. Deparaffinized and rehydrated sections were processed with microwaving in citrate buffer, pH 6.0 for antigen retrieval.

For light microscopic immunohistochemistry, serial 6-μm-thick sections were quenched in 3% hydrogen peroxide, blocked with 5% skim milk/PBS and incubated overnight with rabbit anti-PJA1 (#HPA000595: Atlas Antibodies, Bromma, Sweden; 1:100), mouse monoclonal anti-phosphorylated TDP-43 (#TIP-PTDM01; Cosmo Bio; 1:2000), and rabbit anti-HSF1 (Cell Signaling; #4356) antibodies, followed by incubation with Histofine polymer-immunocomplex (Nichirei, Tokyo, Japan). Immunoreaction was visualized by incubation with 3,3′-diaminobenzidine tetrahydrochloride as the chromogen, and sections were counterstained with hematoxylin and examined under the Olympus AX80TR microscope equipped with a DP70 CCD camera.

For double immunofluorescence, deparaffinized sections were blocked with 10% normal goat serum and incubated overnight with a mixture of rabbit anti-PJA1 (#HPA000595; Atlas Antibodies; 1:50) and mouse monoclonal anti-phosphorylated TDP-43 (#TIP-PTD-M01; Cosmo Bio; 1:2000), followed by incubation with a mixture of Alexa 488-conjugated goat anti-rabbit IgG and Alexa 568-conjugated anti-mouse IgG antibodies (Molecular Probes, Eugene, OR, USA) at a dilution of 1:1000 for 1 h. The sections were treated with Autofluorescence Eliminator Reagent (#2160; Merk Millipore, Burlington, MA, USA) according to manufacturer's instructions to eliminate endogenous lipofuscin autofluorescence, mounted with VECTASHIELD mounting medium with 4′,6-diamidino-2-phenylindole (DAPI) nuclear stain (Vector), and examined under a Carl Zeiss LSM700 confocal laser scanning microscope.

Statistics

Values in each group were expressed as mean ± SD. To compare between two groups, the unpaired Student's t-test and Mann–Whitney's U-test were used for measured results. Values in three to eight groups of measured results were compared by one-way analysis of variance followed by post hoc Bonferroni correction. Statistical significance was considered when P-values were less than 0.05.

RESULTS

HSF1 suppresses cytoplasmic TDP-43 aggregate formation in 1464R neurons

In the present study, we used an adult rat neural stem cell line 1464R that we established to examine aggregate formation of adenovirally-induced TDP-43 as described previously.[8,9,23] The 1464R cells differentiate predominantly (> 80%) into TuJ1-positive neurons and, to a lesser extent (< 20%), into glial fibrillary acidic protein (GFAP)-positive astrocytes and O4-positive oligodendrocytes in the presence of ATRA.[8,9,23] These differentiated 1464R neurons and glial cells formed cytoplasmic aggregates of TDP-43 following co-infection of adenoviruses expressing DsRed-tagged WT and CTF TDP-43 in the presence of proteasome inhibitors.[8,9] These cytoplasmic TDP-43 aggregates were strongly immunoreactive for phosphorylated TDP-43, p62, and ubiquitin, were ultrastructurally composed of non-membrane bound, electron-dense fine granular materials, and were detected in sarkosyl-insoluble or RIPA-insoluble fraction by Western blot analysis, which recapitulates pathological features of TDP-43 aggregates observed in human ALS and FTLD.[8,9]

In this study, we first examined the suppressing effects of an adenovirus expressing HSF1 on adenovirus-induced cytoplasmic TDP-43 aggregate formation in the differentiated 1464R neurons. The 1464R cells were differentiated in the presence of ATRA for 4 days in differentiation medium and infected with adenoviruses expressing DsRed-tagged human WT (AxDsRhWTTDP43) and CTF

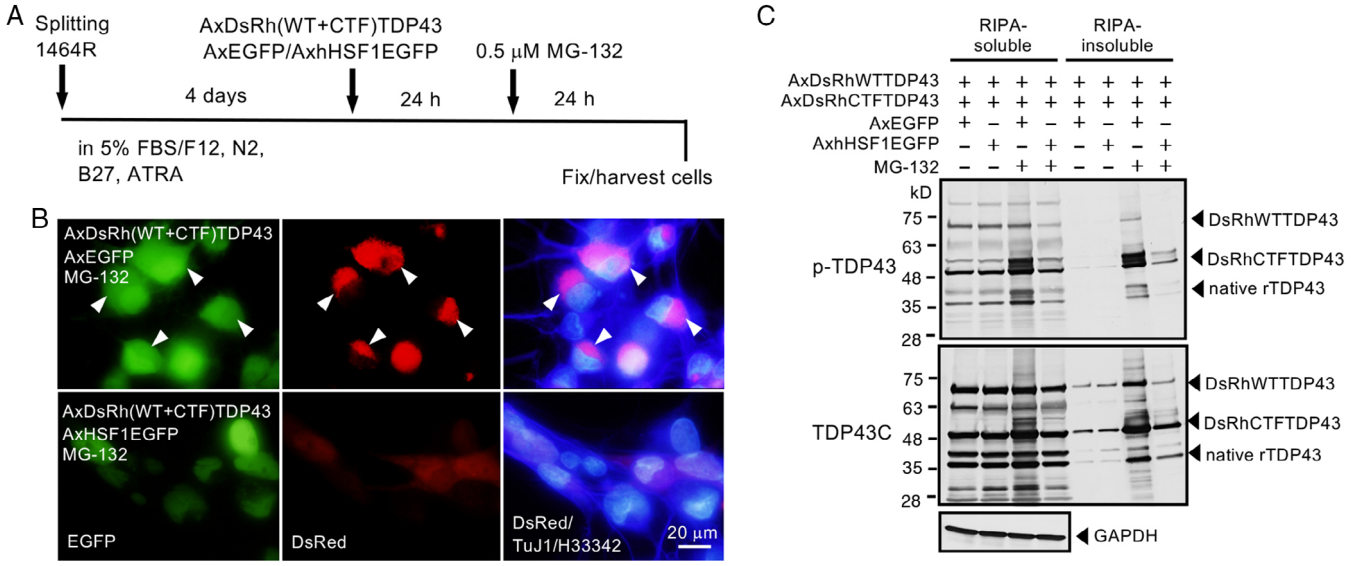

Fig. 1 Suppression of cytoplasmic TDP-43 aggregate formation by HSF1. (A) Schematic presentation of 1464R cell culture experiments for adenoviral TDP-43 aggregate formation. The 1464R cells are cultured in differentiation medium containing all trans retinoic acid (ATRA) and infected with adenoviruses expressing DsRed-tagged human wild-type (WT) (AxDsRhWTTDP43) and CTF (AxDsRhCTFTDP43) TDP-43 and EGFP-tagged human HSF1 (AxhHSF1EGFP) followed by incubation with 0.5 μM MG-132. (B) Fluorescence micrographs showing formation of DsRed-positive dense cytoplasmic aggregates (arrows) in TuJ1-immunoreactive differentiated neurons induced by TDP-43 adenoviruses in the presence of 0.5 μM MG-132 (top row). The TDP-43 aggregate formation is markedly suppressed by co-infection of an EGFP-tagged HSF1 adenovirus (bottom row). Adenoviral HSF1 is localized to nuclei. The nucleus is counterstained with Hoechst 33342. (C) Western blot analysis shows that HSF1 adenovirus infection markedly decreased the amount of adenovirus-induced RIPA-insoluble fractions containing phosphorylated TDP-43.

(AxDsRhCTFTDP43) TDP-43 and EGFP-tagged human HSF1 (AxhHSF1EGFP) in the presence of a proteasome inhibitor MG-132 (Fig. 1A). Fluorescence microscopy revealed formation of DsRed-positive dense cytoplasmic aggregates in TuJ1-immunoreactive differentiated neurons induced by TDP-43 adenoviruses when proteasome activity was inhibited by MG-132. The TDP-43 aggregate formation was suppressed by co-infection of an EGFP-tagged HSF1 adenovirus (Fig. 1B). Western blot analysis demonstrated that HSF1 adenovirus infection markedly decreased the amount of adenovirus-induced RIPA-insoluble fractions containing phosphorylated TDP-43 (Fig. 1C). These results confirmed successful inhibition of cytoplasmic TDP-43 aggregate formation by HSF1 in our adenoviral TDP-43 culture system. It is noteworthy that phosphorylation predominantly occurred in CTF TDP-43 in this culture system, as previously described.[9] This was observed in previous reports and in cases of FTLD-U and ALS patients,[25,26] although the mechanisms involving selective phosphorylation of CTF TDP-43 remain unknown.

DNA microarray analysis of TDP-43 aggregate formation in 1464R-derived neurons

It has been known that HSF1 acts as a master transcriptional regulator of heat shock response and governs expression of hundreds of underling proteins, including those distinct from heat shock.[27] We therefore performed DNA microarray analysis to identify candidate molecules located downstream of HSF1 that counteract TDP-43 aggregate formation. The differentiated 1464R cells were co-infected with adenoviruses expressing WT and CTF hTDP-43, and hHSF1 in the presence of proteasome inhibitor MG-132 with the same protocols as indicated in Fig. 1A. Total RNA were isolated, DNA microarray analysis was performed, and candidate genes were cloned and examined by fluorescence microscopy and Western blot analysis. We found 64 genes that were upregulated more than twofold by HSF1 transduction, and 393 genes that were upregulated more than twofold in association with aggregate inhibition by HSF1 transduction. Notably, genes for most heat shock proteins were not included in these upregulated genes associated with inhibition of TDP-43 aggregate formation by HSF1 transduction. We then selected 50 genes and PCR-cloned them into EGFP-expressing plasmids, transfected these plasmids to 1464R cells, and examined their suppressing effects on adenoviral DsRed-positive TDP-43 aggregate formation under fluorescent microscopy (Fig. 2A); we chose approximately 20 genes expressing EGFP that did not co-localize with adenoviral DsRed-positive TDP-43 aggregates (Fig. 2B) and prepared adenoviruses expressing these genes. We then screened

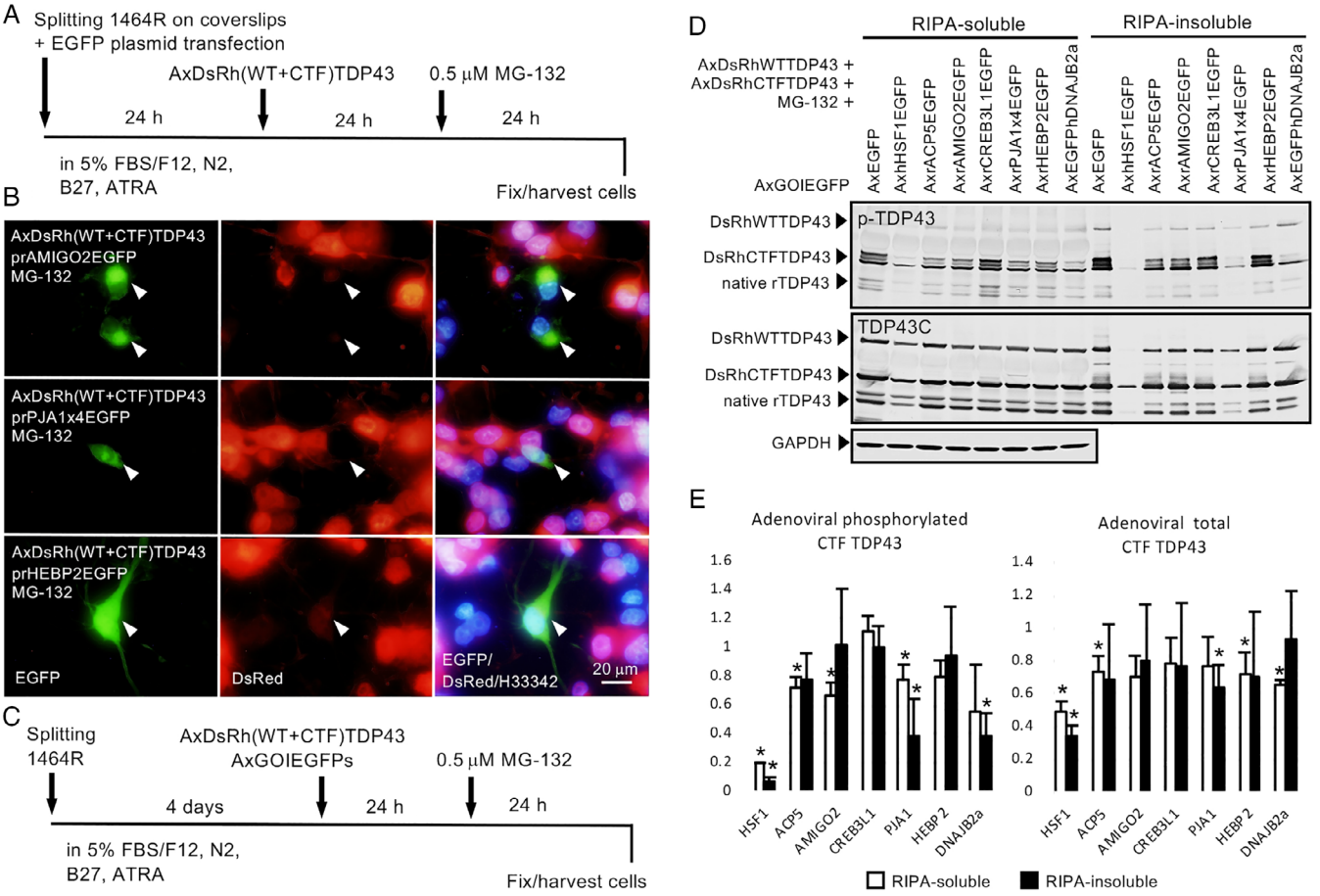

Fig. 2 Screening of candidate genes to suppress TDP-43 aggregate formation in 1464R-derived neurons. (A) Schematic presentation of 1464R cell transfection experiments for the screening of candidate genes. The dissociated 1464R cells on coverslips are immediately transfected with plasmids expressing EGFP-tagged candidate genes followed by TDP-43 adenovirus infection and MG-132 incubation. (B) Fluorescence microscopy of fixed cells expressing EGFP-tagged AMIGO2 (top row), PJA1 (middle row), and HEBP2 (bottom row) that do not contain adenoviral DsRed-positive TDP-43 aggregates. (C) Schematic presentation of 1464R cell culture experiments for screening EGFP-tagged adenoviruses expressing gene of interest (AxGOIEGFPs) to suppress adenoviral TDP-43 aggregate formation. (D) Western blot analysis of suppressive effects of EGFP-tagged adenoviruses expressing ACP5, AMIGO2, CREB3L1, PJA1, HEBP2, and DNAJB2a on adenoviral TDP-43 aggregate formation. (E) Densitometric analysis of the Western blot data of (D) ($n = 3$) calibrated with GADPH signals. Data are expressed as relative density compared with AxEGFP-treated positive control samples. Results are presented as mean ± SD. Statistical comparison is done by two-tailed unpaired *t*-test (*$P < 0.05$). PJA1 and DNAJB2a suppress phosphorylation and aggregate formation of TDP-43.

(Fig. 2C) and narrowed down the candidates that suppress TDP-43 aggregate formation to the following five molecules by fluorescence microscopy and Western blot analysis: acid phosphatase 5, tartrate resistant (ACP5); adhesion molecule with Ig-like domain 2 (AMIGO2); cAMP responsive element binding protein 3-like 1 (CREB3L1); Praja RING-H2 finger E3 ubiquitin ligase 1 (PJA1); and heme binding protein 2 (HEBP2) (Table 1). Western blot analysis using adenoviruses expressing these five molecules showed mild to strong suppressive effects on adenoviral soluble or insoluble TDP-43 expression (Fig. 2D, E). Among these, PJA1 adenovirus definitely suppressed phosphorylation and aggregate formation of TDP-43. Based on Western blot analysis, HSP40/DNAJB2a adenovirus also showed strong suppressive effects on TDP-43 aggregate formation (Fig. 2D), as previously described,[20] although we observe faint induction of DNAJB2a by HSF1 in our DNA microarray analysis (Table 1). We therefore focused on PJA1 protein for further analysis.

PJA1 suppresses phosphorylation and aggregate formation of TDP-43

PJA1 is a RING-H2 finger E3 ubiquitin ligase abundantly expressed in human and rodent brains[28–30] and four types of alternative splicing variants have been identified (Fig. 3A). PJA1 is known to be a short living-protein that

is self-ubiquitinated by its RING-H2 domain and degraded by the proteasome.[31] Consistent with our DNA microarray results as above, we confirmed upregulation of endogenous PJA1 protein induced by adenoviral HSF1, where suppression of ubiquitin-mediated degradation by proteasome inhibitor MG-132 enhanced the detection of native PJA1 bands, predominantly in its shortest form (variant X4), as verified with its migration status by

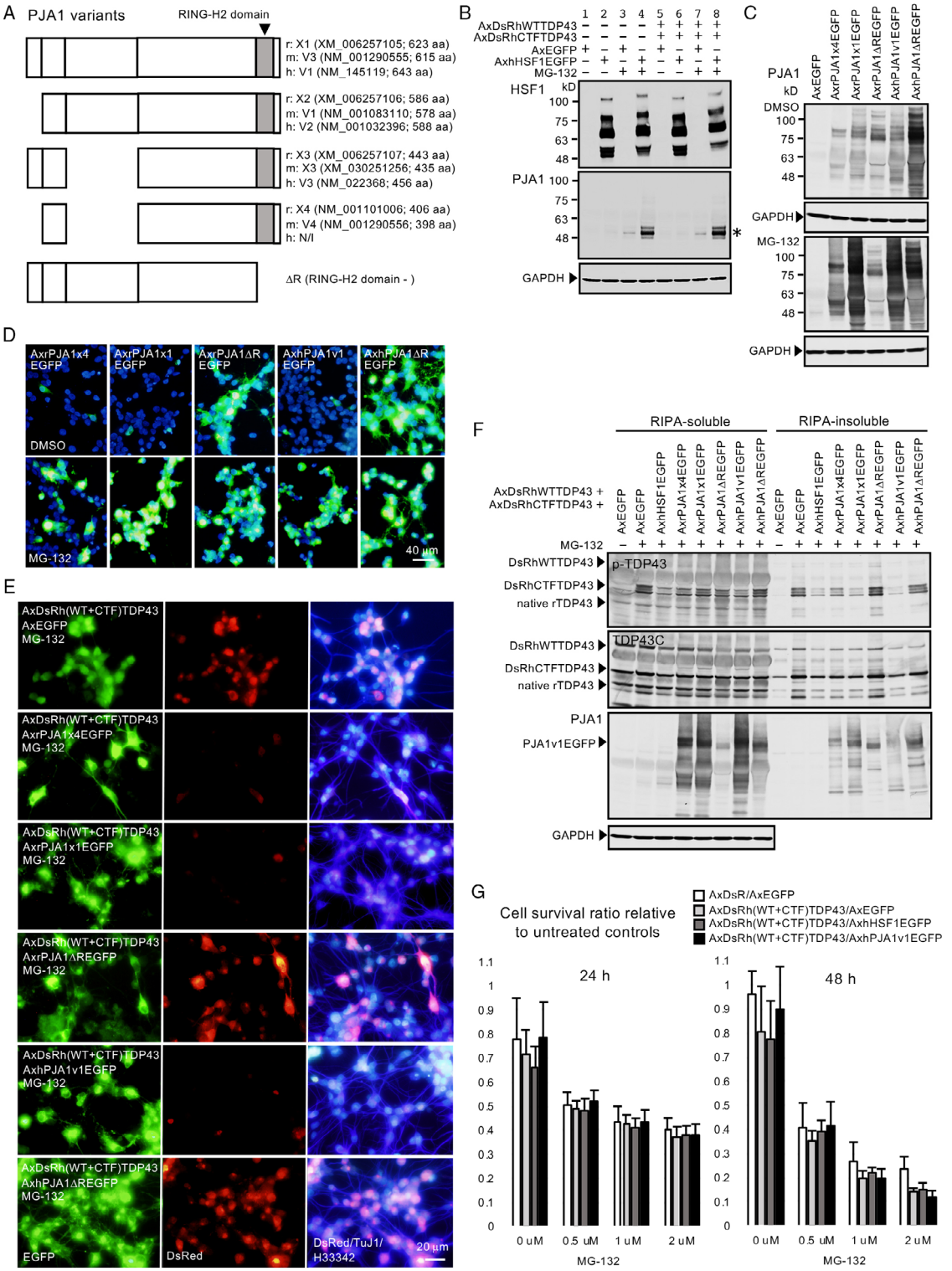

Fig. 3 Legend on next page.

Western blot analysis (Fig. 2B). We constructed PJA1 adenoviruses and examined adenovirally-induced rat and human PJA1 proteins in differentiated 1464R neurons by Western blot (Fig. 3C) and fluorescence microscopy (Fig. 3D, E). We confirmed that adenoviral PJA1 is also self-ubiquitinated by its RING-H2 domain and rapidly degraded by proteasome; deletion of RING-H2 domain (ΔR) stabilized the protein resulting higher expression levels under Western blot and fluorescence microscopic analyses (Fig. 3C, D). In contrast, WT PJA1 adenoviruses strongly suppressed adenoviral TDP-43 phosphorylation and aggregate formation under proteasome inhibition, while PJA1 lacking its RING finger domain (PJA1ΔR) did not show these suppressive effects (Fig. 3E, F). These results indicate that PJA1 controls phosphorylation and proteasomal degradation of TDP-43 in our culture system.

To investigate whether adenoviral expression of HSF1 or PJA1 affects cell survival after adenoviral TDP-43 expression and proteasome inhibition, we performed a cell viability assay using CCK-8 reagent. The results showed no significant difference in cell survival between control, HSF1 and PJA1 groups (Fig. 3G), indicating that inhibition of TDP-43 aggregate formation by HSF1 and PJA1 does not support cell survival in our experimental paradigm.

To exclude the possibility that MG-132 has specific effects on HSF1 and PJA1 function besides proteasome inhibition, we examined other proteasome inhibitors, including lactacystin, epoxomicin, and bortezomib. These proteasome inhibitors equally enhanced formation of RIPA-insoluble phosphorylated TDP-43, which was suppressed by adenoviral PJA1 (Fig. 4A), confirming the common suppressing effects of PJA1 on phosphorylation and aggregate formation of TDP-43 under the condition of proteasome inhibition.

Because it has been shown that induction of autophagy also facilitates suppression of phosphorylation and aggregate formation of TDP-43,[7] we examined the effects of autophagy inhibitors; that is, 3-methyladenine, bafilomycin A1 and wortmannin on adenoviral TDP-43 aggregate formation. Western blot analysis showed none of the significant effects of these inhibitors on TDP-43 aggregate formation nor their antagonizing effects on HSF1 or PJA1 (Fig. 4B), suggesting that protein metabolism of adenoviral TDP-43 aggregate formation in the present experiments is largely controlled by proteasome function. Adenoviral overexpression of PJA1 should, therefore, functionally antagonize proteasomal dysfunction to degrade TDP-43 in its aggregation process in the present study.

In addition, we demonstrated that adenoviral HSF1 lacking its transcriptional activation domain (HSF1Δ [380–529]) and PJA1ΔR are similarly lacking in suppressive effects on TDP-43 phosphorylation and aggregation (Fig. 4C). The HSF1Δ, acting as a dominant-negative form as previously described,[32] blocked HSF1 activity by competing with WT HSF1 to bind target DNA and inhibited the suppressing effects of adenoviral WT HSF1 on TDP-43 aggregate formation (Fig. 4C, lane 2–4). In a similar manner, PJA1ΔR would attenuate the suppressive effects of HSF1 and PJA1 on TDP-43 aggregate formation, provided that PJA1 is a principal factor located downstream of HSF1 that counteract TDP-43 aggregate formation and PJA1ΔR lacking RING-H2 domain acts in a dominant-negative manner to compete with wild-type PJA1 to bind TDP-43. However, in the present study, PJA1ΔR did not act in a dominant-negative

Fig. 3 Suppression of phosphorylation and aggregate formation of TDP-43 by PJA1. (A) Schematic presentation of the primary structure of rat, mouse, and human PJA1. RING-H2 domains located in the C-terminal region are depicted with dark gray boxes. h, human; m, mouse; N/I, not identified; r, rat. (B) Western blot analysis of endogenous PJA1 induction by the HSF1 adenovirus in 1464R cells. The 1464R cells are infected with TDP-43 and HSF1 adenoviruses as indicated in Figure 1A. PJA1 expression is enhanced by adenoviral HSF1 and 0.5 μM MG-132 treatments, predominantly in its shortest form (variant X4; asterisk approximately 50 kD). (C) Western blot analysis of EGFP-tagged adenoviruses expressing rat variant X4 (AxrPJA1x4EGFP), rat variant X1 (AxrPJA1x1EGFP), rat RING-H2-lacking variant X1 (AxrPJA1ΔREGFP), human variant V1 (AxhPJA1v1EGFP), and human RING-H2-lacking variant V1 (AxhPJA1ΔREGFP). Increased expression of wild-type (WT) PJA1 in the presence of 0.5 μM MG-132 is due to inhibition of proteasomal degradation of self-ubiquitinated PJA1, while expression of PJA1 lacking RING-H2 domain is independent of proteasomal activity. (D) EGFP fluorescence of 1464R-derived neurons infected with PJA1EGFP adenoviruses in the absence or presence of MG-132. The nucleus is counterstained with Hoechst 33342. WT PJA1EGFP fluorescence is enhanced in the presence of MG-132 due to proteasomal inhibition, while EGFP expression of PJA1 lacking RING-H2 domain is not affected by MG-132 treatment. (E) Fluorescence microscopy of 1464R-derived neurons infected with adenoviruses expressing DsRed-tagged human WT and CTF TDP-43 and EGFP-tagged PJA1 constructs in the presence of MG-132. Adenoviruses expressing rat and human WT PJA1 (AxrPJA1x4EGFP, AxrPJA1x1EGFP, AxhPJA1v1EGFP) suppress DsRed-positive cytoplasmic TDP-43 aggregate formation, but those lacking RING-H2 domain (AxrPJA1ΔREGFP, AxhPJA1ΔREGFP) do not. (F) Western blot analysis of 1464R-derived neurons infected with adenoviruses expressing DsRed-tagged human WT and CTF TDP-43 and EGFP-tagged HSF1 and PJA1 constructs in the absence or presence of 0.5 μM MG-132. Adenoviruses expressing rat and human HSF1 and WT PJA1 (AxrPJA1x4EGFP, AxrPJA1x1EGFP, AxhPJA1v1EGFP) suppress formation of RIPA-insoluble phosphorylated TDP-43, but those lacking RING-H2 domain (AxrPJA1ΔREGFP, AxhPJA1ΔREGFP) do not. (G) Cell viability assay using CCK-8 reagent. The *y*-axis depicts cell survival ratio relative to untreated control. There was no significant difference in cell survival between EGFP, hHSF1EGFP, and hPJA1v1EGFP adenovirus infections followed by MG-132 treatment, while both longer (48 versus 24 h) incubation and higher (0, 0.5, 1, versus 2 μM) concentration of MG-132 exacerbate the cell survival.

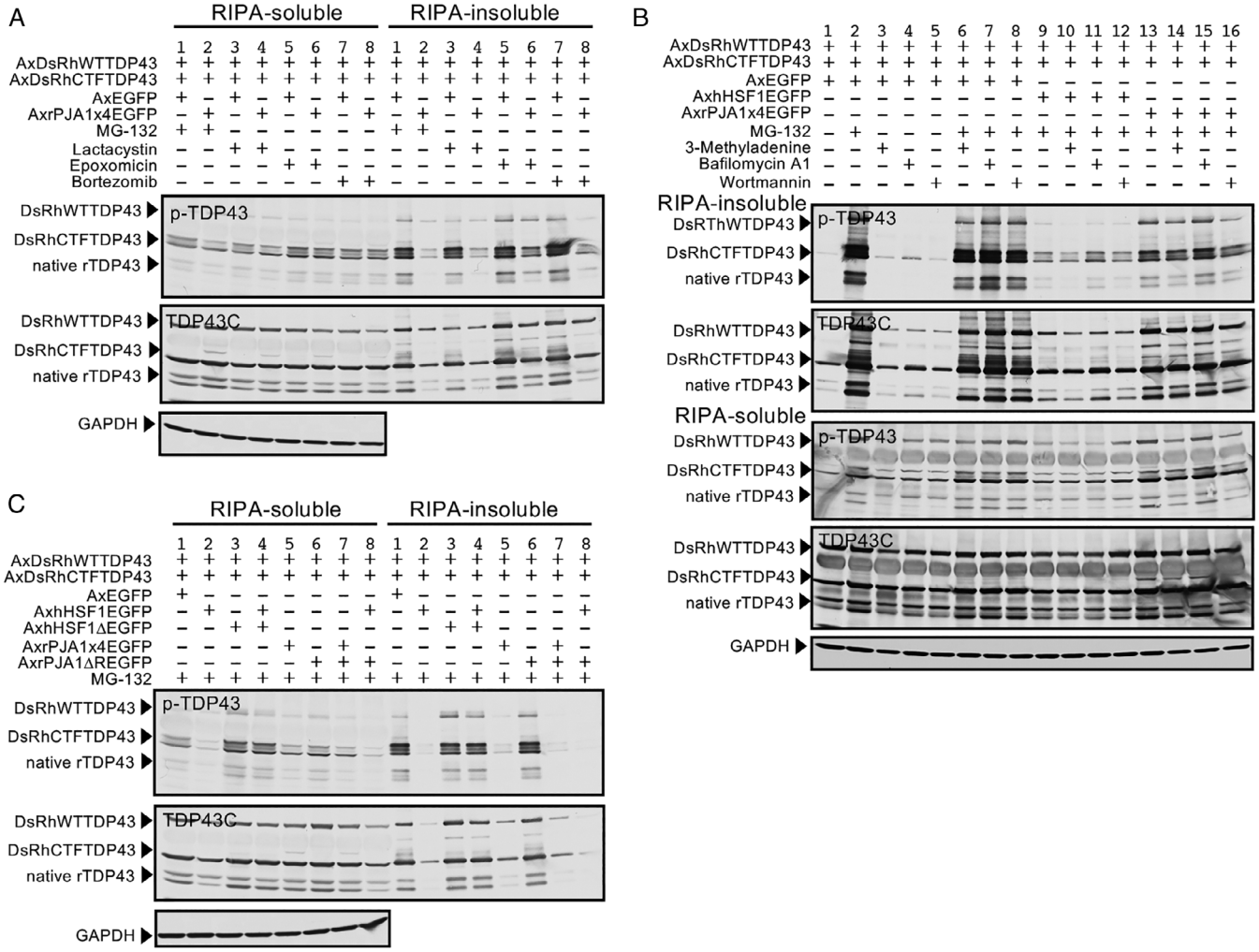

Fig. 4 Suppression of phosphorylation and aggregate formation of TDP-43 by PJA1 via proteasomal degradation. (A) Western blot analysis of suppressive effects of adenoviral PJA1 on phosphorylation and aggregate formation of TDP-43 after wild-type (WT) and CTF TDP-43 adenovirus infection in the absence or presence of proteasome inhibitors MG-132 (0.5 μM), lactacystin (1 μM), epoxomicin (0.1 μM), and bortezomib (0.5 μM). These proteasome inhibitors equally enhance formation of RIPA-insoluble phosphorylated TDP-43, which was suppressed by adenoviral PJA1. (B) Western blot analysis of suppressive effects of adenoviral HSF1 and PJA1 on phosphorylation and aggregate formation of TDP-43 after WT and CTF TDP-43 adenovirus infection in the absence or presence of proteasome inhibitor MG-132 (0.5 μM) and autophagy inhibitors 3-methyladenine (5 mM), bafilomycin A1 (0.1 μM), and wortmannin (1 μM). These autophagy inhibitors give rise to no significant effects on phosphorylation and aggregate formation of TDP-43 (lanes 3–8) nor antagonizing effects on HSF1 or PJA1 (lanes 10–16). (C) Western blot analysis of adenoviruses expressing HSF1 lacking its catalytic domain (HSF1Δ [380–529]) and PJA1ΔR, both of which are defective of suppressive effects on TDP-43 phosphorylation and aggregation (lanes 3, 6). Adenoviral HSF1Δ, acting as a dominant-negative form, inhibits suppressing effects of WT HSF1 on TDP-43 aggregate formation (lane 1–4), while PJA1ΔR does not act in a dominant-negative manner to suppress WT PJA1 or HSF1 function (lane 5–8).

manner to suppress WT PJA1 or HSF1 function (Fig. 4C, lanes 5–8); whether PJA1 is an exclusively dominant effector molecule located downstream of HSF1 that counteracts TDP-43 aggregate formation remains elusive.

PJA1 binds to TDP-43 and E2 ubiquitin conjugating enzyme UBE2E3

We next examined whether PJA1 binds to and ubiquitinates TDP-43. We constructed adenoviruses expressing DsRed (on 5′-end)-tagged and FLAG (on 3′-end)-tagged TDP-43 WT and CTF for Co-IP experiments. The CTF TDP-43 adenovirus preferably induced RIPA-insoluble phosphorylated TDP-43, and the adenovirally induced PJA1 is also consistently localized in both RIPA-soluble and insoluble fractions (Fig. 5A) as described above (Fig. 3F). The Co-IP assay revealed that adenoviral PJA1 preferentially binds to CTF TDP-43 (Fig. 5B; Lanes 5, 7), while CTF TDP-43 was consistently ubiquitinated irrespective of adenoviral PJA1

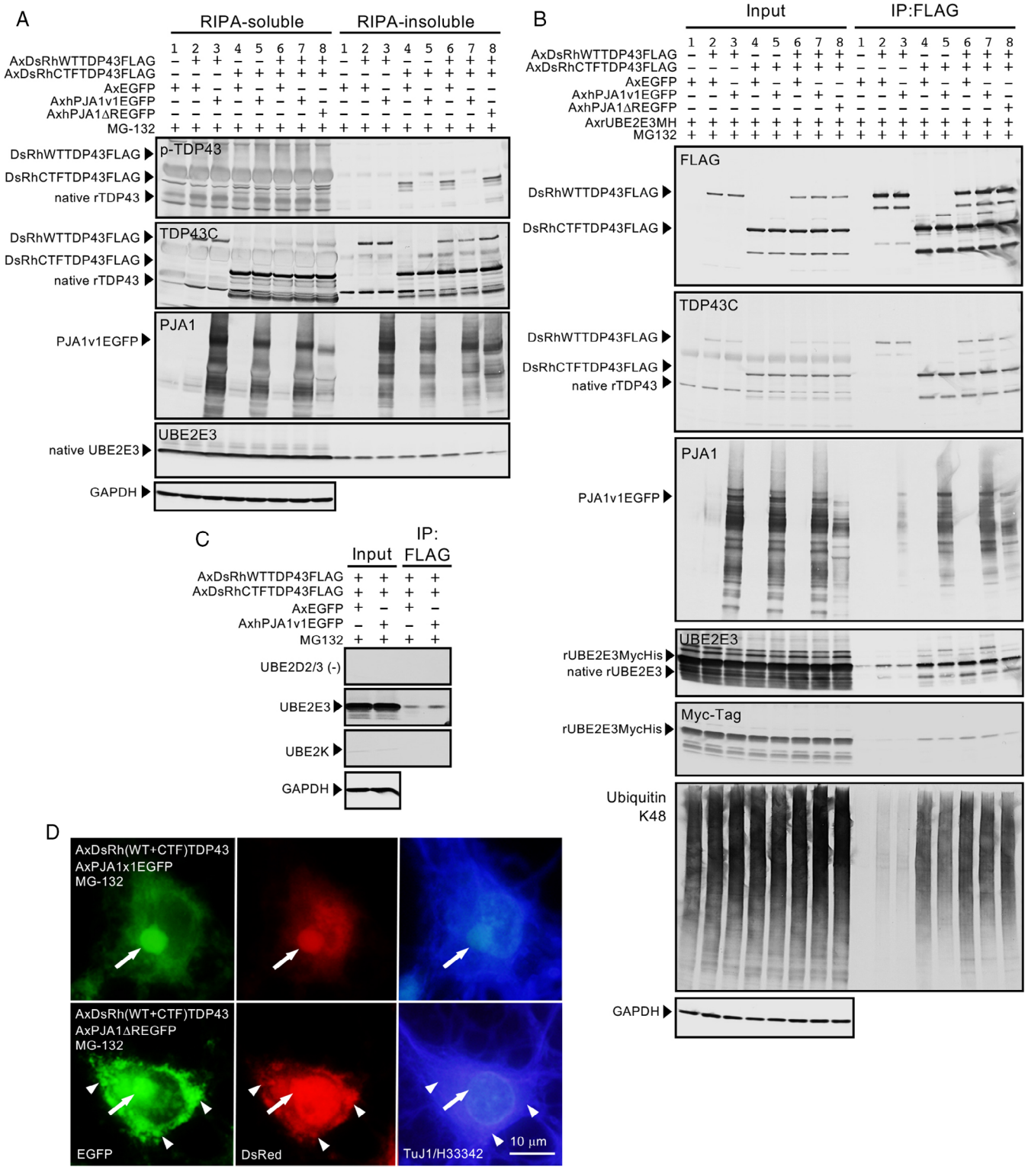

Fig. 5 Legend on next page.

overexpression (Fig. 5B; ubiquitin K48 Western blot analysis, lanes 4-8), probably due to concomitant presence of endogenous PJA1 and/or other unidentified E3 enzymes to ubiquitinate CTF TDP-43 in this Co-IP preparation. Because it has been reported that PJA1 works robustly with the E2-conjugating enzymes UBE2D2/3, UBE2E3, and UBE2K,[33] we examined E2 enzymes in Co-IP assay by Western blot and found that

both endogenous and adenovirally-induced UBE2E3 were co-immunoprecipitated with TDP-43 and PJA1 (Fig. 5B, C), which strongly suggests that UBE2E3 is a preferential partner of PJA1 to ubiquitinate TDP-43.

Fluorescence microscopic observation of differentiated 1464R neurons infected with DsRed-tagged TDP-43 and EGFP-tagged PJA1 also revealed co-localization of cytoplasmic TDP-43 and PJA1. Higher magnification showed two types of co-localization; that is, perinuclear round fluorescence and cytoplasmic amorphous aggregates (Fig. 5D). The former perinuclear fluorescence appeared to localize to stress granules[34–37] found in cells infected with adenovirus expressing both WT and RING finger domain lacking (ΔR) PJA1, while the latter cytoplasmic aggregates were observed only in cells expressing PJA1ΔR adenovirus, which would be degraded by WT PJA1 (Fig. 5D). These fluorescence results suggest that PJA1 binds to TDP-43 in stress granules and suppresses the formation of cytoplasmic TDP-43 aggregates.

PJA1 suppresses TDP-43 aggregate formation in mouse facial motor neurons *in vivo*

To investigate the suppressive effects of adenoviral HSF1 and PJA1 expression on TDP-43 aggregate formation in adult mouse motor neurons *in vivo*, we co-injected DsRed/TDP-43 (WT + CTF), HSF1/EGFP and PJA1/EGFP adenoviruses into the facial nerve and let the viruses transfer to the facial motor neurons via retrograde axonal transport, and express the virus-induced foreign genes in the motor neurons (Fig. 6). After the adenovirus injection (n = 4), 50–60% of mouse facial motor neurons were strongly labeled with DsRed and/or EGFP, which is much more efficient than rat facial motor neurons (10–30% labeled), as observed in our previous study.[8] In the current mouse experiments, 30–40% of DsRed/TDP-43 (WT + CTF)-labeled motor neurons contained DsRed-positive cytoplasmic granular aggregates without proteasome inhibition (Fig. 6A, D). This was performed in previous experiments with rats,[8] but probably due to the much higher transduction efficiency of adenoviral TDP-43 in mice, the degrading capacity of endogenous proteasome function was more overwhelmed than in rats. These mouse motor neurons bearing cytoplasmic aggregates were significantly decreased to <10% by co-infection of HSF1 or PJA1 adenovirus (Fig. 6B–D). The cells bearing cytoplasmic DsRed/TDP-43 aggregates partially colocalized to PJA1/EGFP fluorescence are infrequently observed (Fig. 6C), which may represent the degrading process of DsRed/TDP-43 by PJA1/EGFP. Together with the cell culture experiments as described above, the present study indicates the significant suppressive effect of PJA1 on TDP-43 aggregate formation both *in vitro* and *in vivo*.

Phosphorylated TDP-43 aggregates in PJA1-immunoreactive human amyotrophic lateral sclerosis motor neurons

Finally, we examined expression of PJA1 in motor neurons of human control and ALS spinal cords. Serial lumbar spinal cord sections were immunostained with PJA1, phosphorylated TDP-43, and HSF1. In non-diseased control cases, the great majority of neuronal cells that include spinal motor neurons were constitutively immunoreactive for PJA1 and HSF1 but not for phosphorylated TDP-43 (Fig. 7A–C). In ALS cases, cytoplasmic round inclusions immunoreactive for phosphorylated TDP-43 were observed in PJA1- and HSF1-immunopositive atrophic spinal motor neurons (Fig. 7D, E). Double immunofluorescence staining demonstrated cytoplasmic round and skein-like inclusions immunoreactive for phosphorylated TDP-43 in PJA1-immunoreactive ALS motor neurons, although these inclusions were not immunostained for PJA1 (Fig. 7G–L).

DISCUSSION

We have previously demonstrated adenovirally-induced TDP-43 cytoplasmic aggregate formation in 1464R-

Fig. 5 PJA1 binding to TDP-43 and E2 ubiquitin conjugating enzyme UBE2E3. (A) Western blot analysis of suppressive effects of adenovirus expressing human PJA1v1, but not PJA1ΔR, on phosphorylation and aggregate formation of TDP-43 after DsRed- and FLAG-tagged wild-type (WT) and CTF TDP-43 adenovirus infection in the presence of 0.5 μM MG-132 (lanes 3–8). The CTF TDP-43 adenovirus preferably induces RIPA-insoluble phosphorylated TDP-43 (lanes 4, 6). Adenovirally-induced hPJA1v1 and hPJA1ΔR is consistently localized in both RIPA-soluble and insoluble fractions (lanes 3, 5, 7, 8), and adenoviral hPJA1v1, but not hPJA1ΔR, decreases RIPA-insoluble phosphorylated CTF TDP-43 (lanes 5, 7) in a similar manner to the experiment shown in Figure 3F. Endogenous UBE2E3 is also detected both in RIPA-soluble and insoluble fractions. (B) The co-immunoprecipitation (Co-IP) assay shows that PJA1 preferentially binds to CTF TDP-43 rather than WT TDP-43 (PJA1 blot; lanes 3, 5, 7, 8), while CTF TDP-43 is consistently ubiquitinated irrespective of adenoviral PJA1 induction (Ubiquitin K48 blot; lanes 4–8). Both native and adenoviral UBE2E3 are co-immunoprecipitated with WT and CTF TDP-43 (UBE2E3 and Myc-Tag blots). (C) Co-IP assay indicates that TDP-43 and/or PJA1 bind to UBE2E3 but not UBE2D2/3 or UBE2K. (D) Fluorescence micrographs of TuJ1-immunoreactive differentiated neurons co-infected with DsRed-tagged WT and CTF TDP-43 adenoviruses and EGFP-tagged hPJA1v1 (top row) or hPJA1ΔR (bottom row) adenovirus in the presence of 0.5 μM MG-132. The nucleus is counterstained with Hoechst 33342. Two types of co-localization (i.e., perinuclear round fluorescence [arrows] and cytoplasmic amorphous aggregates [arrowheads]), are observed.

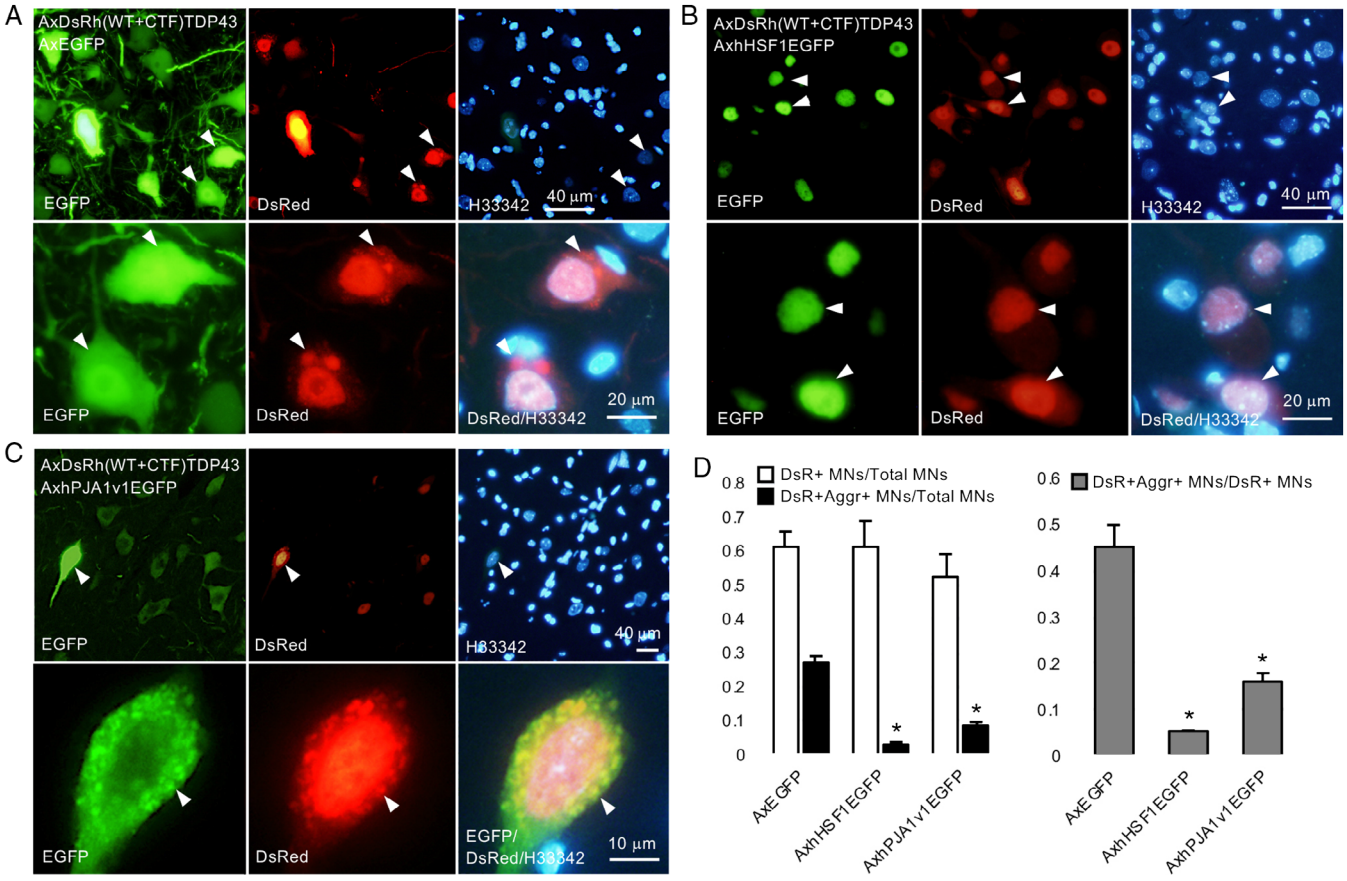

Fig. 6 Suppression of TDP-43 aggregate formation by HSF1 and PJA1 in adult mouse facial motor neurons *in vivo*. Adult mouse facial motor neurons are infected with DsRed-tagged wild-type (WT) and CTF TDP-43 adenoviruses and EGFP (A), hHSF1EGFP (B), or hPJAv1EGFP (C) adenovirus by retrograde transport after facial nerve injection ($n = 4$). The nucleus is counterstained with Hoechst 33342. (A) Cytoplasmic aggregates (arrowheads) are formed by WT and CTF TDP-43 adenovirus infection. (B) Co-infection of hHSF1/EGFP adenovirus increases cells devoid of cytoplasmic TDP-43 aggregates (arrowheads). (C) Co-infection of hPJA1/EGFP adenovirus also attenuates cells bearing cytoplasmic TDP-43 aggregates. Cells bearing cytoplasmic DsRed/TDP-43 aggregates partially colocalized to PJA1/EGFP fluorescence are infrequently observed (arrowheads). Immunofluorescence for GFP is performed to enhance detection of PJA1/EGFP as described in the text. (D) Percentages of DsR+ and DsR+/aggregate+ motor neurons in H33342-labeled total motor neurons (left graphs) and of DsR+/aggregate+ motor neurons in DsR+ motor neurons (right graphs). Results are presented as mean ± SD ($n = 4$). Statistical comparison is done by Mann–Whitney *U*-test. $^*P < 0.05$ *vs* AxEGFP-treated group.

derived neuronal and glial cells under proteasome inhibition,[8] and established time-lapse imaging analysis of these 1464R cells.[9] The 1464R cell line can be cultured for more than 50 passages with no obvious morphological alterations and, in the presence of ATRA, ceases dividing and differentiates into neuronal and glial cells that recapitulate primary cultured brain cells. Most of these differentiated cells formed insoluble cytoplasmic TDP-43 aggregates that were phosphorylated and ubiquitinated and consisted of electron-dense granules when the cells were treated with proteasome inhibitor MG-132 following adenoviral transduction with WT and CTF TDP-43.[8,9] Time-lapse imaging analyses revealed growing cytoplasmic aggregates in the transduced neuronal and glial cells, followed by collapse of the cell.[9]

In the present study, we observed remarkable suppressing effects of adenoviral HSF1 overexpression on TDP-43 aggregate formation in 1464R-derived neurons, confirming previous reports.[15,20] To investigate candidate molecules locating downstream of HSF1, we performed DNA microarray analysis of TDP-43 aggregate formation using adenovirus-induced 1464R cultures. Unexpectedly, we failed to verify known heat shock proteins that include HSP70,[15] HSPB8,[16–19] and HSP40/DNAJB2a[20] as potential suppressors of TDP-43 aggregate formation in our DNA microarray analysis. In contrast, we found PJA1 E3 ubiquitin ligase to be the most promising molecule to counteract TDP-43 aggregate formation, although adenoviral overexpression of PJA1, as well as HSF1, does not support cell survival in our experimental paradigm.

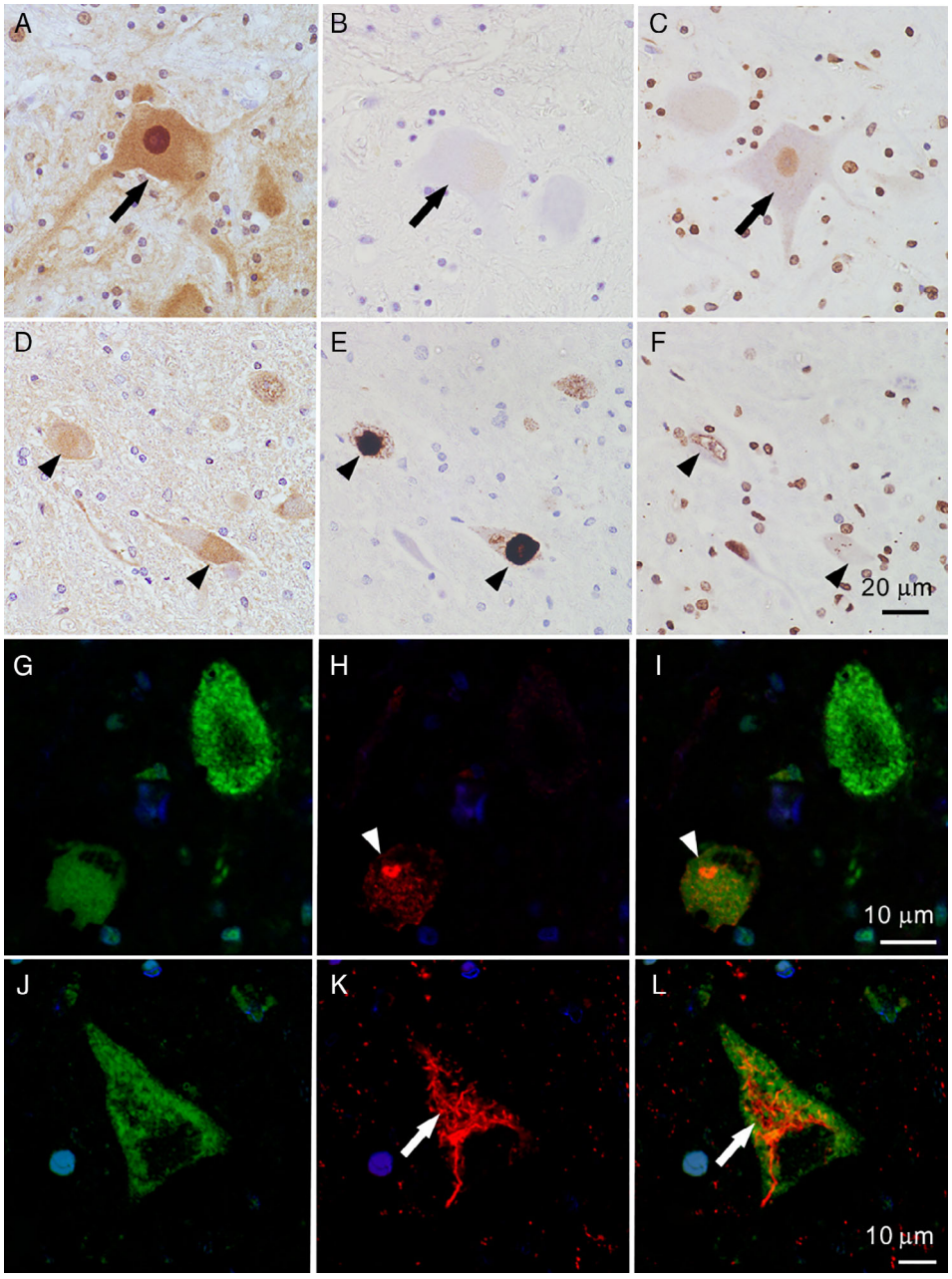

Fig. 7 Phosphorylated TDP-43 aggregates in PJA1-immunoreactive ALS motor neurons. (A-F) Immunohistochemistry of serial sections of lumbar spinal cord of non-diseased control (A-C) and ALS (D-F) cases immunostained for PJA1 (A, D), phosphorylated TDP-43 (B, E), and HSF1 (C, F) reveals that both control (A-C; arrows) and ALS motor neurons bearing phosphorylated TDP-43-positive cytoplasmic inclusions/aggregates (D-F; arrowheads) are immunoreactive for PJA1 (A, D). (G-H) Double immunofluorescence of PJA1 (G, J) and phosphorylated TDP-43 (H, K) of ALS motor neurons bearing cytoplasmic round (G-I; arrowheads) and skein-like (J-L; arrows) inclusions reveals no colocalization of these inclusions to PJA1 immunolabeling. The nucleus is counterstained with DAPI.

PJA1 has been identified as a RING-H2 finger E3 ubiquitin ligase abundantly expressed in the brain, and was initially reported to bind to MAGED1/NRAGE/Dlxin1 *in vitro* and *in vivo*.[28-30] Subsequently, PJA1 has been shown to impair the TGF-β/SMAD signaling-dependent tumor-suppressing pathway in diverse cancer cell lines[38,39] and promote tumorigenesis of glioblastoma cell lines by degrading a transcriptional repressor CIC,[40] while PJA1 promotes skeletal myogenesis through degradation of enhancer of zeste homologue 2 (EZH2).[41] PJA1 has also been described to be upregulated in amygdala during the formation of fear memory,[42] and is suggested to be one of the deleted genes in craniofrontonasal syndrome.[43] However, there have been no reports concerning the association of PJA1 with neurodegenerative disorders, although Neurodap1 showing structural similarity to PJA1 was downregulated after facial nerve axotomy.[44] In addition, although PJA1 was reported to suppress replication of DNA viruses such as hepatitis B virus (HBV) and herpes simplex virus 1 (HSV-1),[45] PJA1 adenoviruses apparently did not suppress replication of all the recombinant adenoviruses including themselves used in the present study.

In this study, we demonstrated that PJA1 binds to TDP-43 and E2 ubiquitin-conjugating enzyme UBE2E3 and suppresses formation of cytoplasmic TDP-43 aggregates, which strongly suggests that PJA1 ubiquitinates and degrades TDP-43 through the ubiquitin-proteasome pathway, although whether PJA1 undoubtedly ubiquitinates TDP-43 awaits further investigation, such as through *in vitro* ubiquitination assay using purified PJA1 and TDP-43 proteins. Several reports have previously described ubiquitinating enzymatic activities against TDP-43. Parkin ubiquitinates TDP-43, but conversely promotes cytoplasmic TDP-43 aggregate formation.[46] Uchida et al. described how the von Hippel Lindau (VHL)/cullin-2 (CUL2) E3 complex ubiquitinates misfolded TDP-43 and promoted clearance of fragmented forms of TDP-43.[47] More recently, Znf-179 E3 ubiquitin ligase was shown to ubiquitinate TDP-43 and attenuate insoluble pathologic TDP-43 aggregates.[48] Interestingly, Hans et al. has previously described UBE2E3 as the E2 conjugating enzyme for TDP-43,[49] although the E3 ligase was not identified in their report. PJA1 as demonstrated in the present study might have been the E3 ligase missing in their report. In addition, we observed two types of co-localization of TDP-43 and PJA1 under fluorescence microscopy: perinuclear round fluorescence putatively representing stress granules[34–37] and cytoplasmic amorphous fluorescence found only in cells infected with PJA1ΔR adenovirus, which were considered to be degraded by WT PJA1. We speculate that PJA1 binds to TDP-43 in stress granules and suppresses the formation of cytoplasmic TDP-43 aggregates, which should be investigated further using stress granule markers to identify co-localization of PJA1 and TDP-43 in these structures.

We also investigated *in vivo* suppressive effects of HSF1 and PJA1 on TDP-43 aggregate formation in adult mouse facial motor neurons by means of retrograde transport of recombinant adenoviruses injected into facial nerves as described previously in rats.[8] We observed significant suppressive effects of both HSF1 and PJA1 adenoviruses on cytoplasmic TDP-43 aggregate formation in adult mouse motor neurons *in vivo*, again indicating that PJA1 as well as HSF1 plays a prominent role in ameliorating cytoplasmic TDP-43 aggregate formation in adult motor neurons *in vivo*. It has been suggested that HSF1 activity is reduced in affected spinal cord in patients with sporadic ALS, which leads to enhanced accumulation and aggregation of TDP-43 in ALS patients.[20] Furthermore, we observed that, in humans, the great majority of neurons that include spinal motor neurons were immunoreactive for PJA1, and, in ALS spinal cord, phosphorylated TDP-43-immunoreactive cytoplasmic round and skein-like inclusions/aggregates were observed in PJA1-immunoreactive motor neurons, although co-localization of PJA1 in these inclusions/aggregates was not demonstrated. These results may indicate that PJA1 is constitutively expressed in the motor neurons where cytoplasmic TDP-43 aggregates are formed, and fully developed cytoplasmic TDP-43 aggregates such as round and skein-like inclusions are no longer the targets of PJA1-initiated proteasomal degradation machinery, although whether PJA1 counteracts development of TDP-43 oligomers or more mature cytoplasmic aggregates awaits further investigation. However, because TDP-43 is ubiquitously expressed in all cells, PJA1 binding to TDP-43 may not be specific to certain neuronal species that include motor neurons or hippocampal granule cells in that cytoplasmic TDP-43 aggregates are predominantly observed in ALS and FTLD cases. We are still unable to explain what causes the cell type specificity of cytoplasmic accumulation and aggregation of TDP-43, which may attribute to the cell type-specific microenvironment harboring aggregation-prone protein species.

There is accumulating evidence that shows that the transmission of pathological aggregates such as amyloid β, tau, α-synuclein, huntingtin, and TDP-43, is the principal causative event in the progression of Alzheimer's disease, Parkinson's disease, Huntington's disease, ALS, and FTLD, respectively.[10–12] This notion is recognized as prion-like propagation, and cell-to-cell spreading of TDP-43 aggregates is a plausible hypothesis for explaining the progressive nature of neurodegeneration observed in ALS and FTLD. It is, therefore, noteworthy that the suppressing effect of PJA1 on formation of TDP-43 aggregates may halt disease progression of ALS and FTLD, while PJA1 did not support cell survival under proteasome inhibition in the present study. In contrast, use of ubiquitin ligase inhibitors has been shown to be an effective strategy in human cancer therapy.[50] Recent reports also described a strategy to discover activators of E3 ligases with ubiquitin variants,[51] which may be attractive therapeutic candidates for neurodegenerative diseases, including ALS and FTLD.

In summary, we performed DNA microarray analysis of the suppressing effect of HSF1 on TDP-43 aggregate formation in rat 1464R-derived neuronal cells. One of the upregulated candidate molecules, PJA1, has a significant capability of suppressing phosphorylation and aggregate formation of TDP-43 *in vitro* and *in vivo*, which may have therapeutic potential in ALS and FTLD.

ACKNOWLEDGMENTS

We are grateful to Mizuho Karita, Hideyuki Takeiri, and Yuko Miyaguchi for technical support. This work was supported by Grants-in-Aid for Scientific Research from the Ministry of Education, Culture, Sports, Science, and Technology, Japan (JSPS KAKENHI) #15 K06763 and #18 K06507 (to KW), and by the Collaborative Research Project (2017-2019) of Brain Research Institute, Niigata University.

DISCLOSURE

The authors declare no competing financial interests.

REFERENCES

1. Blokhuis AM, Groen EJ, Koppers M, van den Berg LH, Pasterkamp RJ. Protein aggregation in amyotrophic lateral sclerosis. *Acta Neuropathol* 2013; **125**: 777–794.
2. Taylor JP, Brown RH Jr, Cleveland DW. Decoding ALS: From genes to mechanism. *Nature* 2016; **539**: 197–206.
3. Berning BA, Walker AK. The pathobiology of TDP-43 C-terminal fragments in ALS and FTLD. *Front Neurosci* 2019; **13**: 335.
4. Hergesheimer RC, Chami AA, de Assis DR *et al*. The debated toxic role of aggregated TDP-43 in amyotrophic lateral sclerosis: A resolution in sight? *Brain* 2019; **142**: 1176–1194.
5. Prasad A, Bharathi V, Sivalingam V, Girdhar A, Patel BK. Molecular mechanisms of TDP-43 misfolding and pathology in amyotrophic lateral sclerosis. *Front Mol Neurosci* 2019; **12**: 25.
6. Robberecht W, Philips T. The changing scene of amyotrophic lateral sclerosis. *Nat Rev Neurosci* 2013; **14**: 248–264.
7. Scotter EL, Vance C, Nishimura AL *et al*. Differential roles of the ubiquitin proteasome system and autophagy in the clearance of soluble and aggregated TDP-43 species. *J Cell Sci* 2014; **127**: 1263–1278.
8. Watabe K, Akiyama K, Kawakami E *et al.* Adenoviral expression of TDP-43 and FUS genes and shRNAs for protein degradation pathways in rodent motoneurons *in vitro* and in vivo. *Neuropathology* 2014; **34**: 83–98.
9. Ishii T, Kawakami E, Endo K, Misawa H, Watabe K. Formation and spreading of TDP-43 aggregates in cultured neuronal and glial cells demonstrated by time-lapse imaging. *PLoS One* 2017; **12**: e0179375.
10. Brettschneider J, Del Tredici K, Lee VM, Trojanowski JQ. Spreading of pathology in neurodegenerative diseases: A focus on human studies. *Nat Rev Neurosci* 2015; **16**: 109–120.
11. Jucker M, Walker LC. Propagation and spread of pathogenic protein assemblies in neurodegenerative diseases. *Nat Neurosci* 2018; **21**: 1341–1349.
12. Peng C, Trojanowski JQ, Lee VM. Protein transmission in neurodegenerative disease. *Nat Rev Neurol* 2020; **16**: 199–212.
13. Dayalan Naidu S, Dinkova-Kostova AT. Regulation of the mammalian heat shock factor 1. *FEBS J* 2017; **284**: 1606–1627.
14. Gomez-Pastor R, Burchfiel ET, Thiele DJ. Regulation of heat shock transcription factors and their roles in physiology and disease. *Nat Rev Mol Cell Biol* 2018; **19**: 4–19.
15. Lin PY, Folorunso O, Taglialatela G, Pierce A. Overexpression of heat shock factor 1 maintains TAR DNA binding protein 43 solubility via induction of inducible heat shock protein 70 in cultured cells. *J Neurosci Res* 2016; **682**: 671–682.
16. Crippa V, Cicardi ME, Ramesh N *et al*. The chaperone HSPB8 reduces the accumulation of truncated TDP-43 species in cells and protects against TDP-43-mediated toxicity. *Hum Mol Genet* 2016; **25**: 3908–3924.
17. Crippa V, D'Agostino VG, Cristofani R *et al*. Transcriptional induction of the heat shock protein B8 mediates the clearance of misfolded proteins responsible for motor neuron diseases. *Sci Rep* 2016; **6**: 22827.
18. Cristofani R, Crippa V, Vezzoli G *et al*. The small heat shock protein B8 (HSPB8) efficiently removes aggregating species of dipeptides produced in C9ORF72-related neurodegenerative diseases. *Cell Stress Chaperones* 2018; **23**: 1–12.
19. Ganassi M, Mateju D, Bigi I *et al*. A surveillance function of the HSPB8-BAG3-HSP70 chaperone complex ensures stress granule integrity and dynamism. *Mol Cell* 2016; **63**: 796–810.
20. Chen HJ, Mitchell JC, Novoselov S *et al*. The heat shock response plays an important role in TDP-43 clearance: Evidence for dysfunction in amyotrophic lateral sclerosis. *Brain* 2016; **139**:1417–1432.
21. Wang P, Wander CM, Yuan CX, Bereman MS, Cohen TJ. Acetylation-induced TDP-43 pathology is suppressed by an HSF1-dependent chaperone program. *Nat Commun* 2017; **8**: 82.
22. Gregory JM, Whiten DR, Brown RA *et al*. Clusterin protects neurons against intracellular proteotoxicity. *Acta Neuropathol Commun* 2017; **5**: 81.
23. Ishii T, Kawakami E, Endo K, Misawa H, Watabe K. Myelinating cocultures of rodent stem cell line-derived neurons and immortalized Schwann cells. *Neuropathology* 2017; **37**: 475–481.
24. Kawai S, Takagi Y, Kaneko S, Kurosawa T. Effect of three types of mixed anesthetic agents alternate to ketamine in mice. *Exp Anim* 2011; **60**: 481–487.
25. Hasegawa M, Arai T, Nonaka T *et al*. Phosphorylated TDP-43 in frontotemporal lobar degeneration and amyotrophic lateral sclerosis. *Ann Neurol* 2008; **64**: 60–70.
26. Igaz LM, Kwong LK, Chen-Plotkin A *et al*. Expression of TDP-43 C-terminal fragments in vitro recapitulates pathological features of TDP-43 proteinopathies. *J Biol Chem* 2009; **284**: 8516–8524.
27. Mendillo ML, Santagata S, Koeva M *et al*.. HSF1 drives a transcriptional program distinct from heat

shock to support highly malignant human cancers. *Cell* 2012; **150**: 549–562.
28. Mishra L, Tully RE, Monga SP *et al*. Praja1, a novel gene encoding a RING-H2 motif in mouse development. *Oncogene* 1997; **15**: 2361–2368.
29. Sasaki A, Masuda Y, Iwai K, Ikeda K, Watanabe K. A RING finger protein Praja1 regulates Dlx5-dependent transcription through its ubiquitin ligase activity for the Dlx/Msx-interacting MAGE/Necdin family protein, Dlxin-1. *J Biol Chem* 2002; **277**: 22541–22546.
30. Yu P, Chen Y, Tagle DA, Cai T. PJA1, encoding a RING-H2 finger ubiquitin ligase, is a novel human X chromosome gene abundantly expressed in brain. *Genomics* 2002; **79**: 869–874.
31. Zoabi M, Sadeh R, de Bie P, Marquez VE, Ciechanover A. PRAJA1 is a ubiquitin ligase for the polycomb repressive complex 2 proteins. *Biochem Biophys Res Commun* 2011; **408**: 393–398.
32. Voellmy R. Dominant-positive and dominant-negative heat shock factors. *Methods* 2005; **35**: 199–207.
33. Loch CM, Eddins MJ, Strickler JE. Protein microarrays for the identification of praja1 E3 ubiquitin ligase substrates. *Cell Biochem Biophys* 2011; **60**: 127–135.
34. Aulas A, Vande Velde C. Alterations in stress granule dynamics driven by TDP-43 and FUS: A link to pathological inclusions in ALS? *Front Cell Neurosci* 2015; **9**: 423.
35. Chen Y, Cohen TJ. Aggregation of the nucleic acid-binding protein TDP-43 occurs via distinct routes that are coordinated with stress granule formation. *J Biol Chem* 2019; **294**: 3696–3706.
36. Wolozin B, Ivanov P. Stress granules and neurodegeneration. *Nat Rev Neurosci* 2019; **20**: 649–666.
37. Loganathan S, Lehmkuhl EM, Eck RJ, Zarnescu DC. To Be or Not To Be … Toxic-Is RNA association with TDP-43 complexes deleterious or protective in neurodegeneration? *Front Mol Biosci* 2020; **6**: 154.
38. Saha T, Vardhini D, Tang Y *et al*. RING finger-dependent ubiquitination by PRAJA is dependent on TGF-beta and potentially defines the functional status of the tumor suppressor ELF. *Oncogene* 2006; **25**: 693–705.
39. Chen J, Mitra A, Li S *et al*. Targeting the E3 ubiquitin ligase PJA1 enhances tumor-suppressing TGF-β signaling. *Cancer Res* 2020 https://doi.org/10.1158/0008-5472.CAN-19-3116, **80**, 1819, 1832.
40. Bunda S, Heir P, Metcalf J *et al*. CIC protein instability contributes to tumorigenesis in glioblastoma. *Nat Commun* 2019; **10**: 661.
41. Consalvi S, Brancaccio A, Dall'Agnese A, Puri PL, Palacios D. Praja1 E3 ubiquitin ligase promotes skeletal myogenesis through degradation of EZH2 upon p38α activation. *Nat Commun* 2017; **8**: 13956.
42. Stork O, Stork S, Pape HC, Obata K. Identification of genes expressed in the amygdala during the formation of fear memory. *Learn Mem* 2001; **8**: 209–219.
43. Wieland I, Weidner C, Ciccone R *et al*. Contiguous gene deletions involving EFNB1, OPHN1, PJA1 and EDA in patients with craniofrontonasal syndrome. *Clin Genet* 2007; **72**: 506–516.
44. Nakayama M, Miyake T, Gahara Y, Ohara O, Kitamura T. A novel RING-H2 motif protein down-regulated by axotomy: Its characteristic localization at the postsynaptic density of axosomatic synapse. *J Neurosci* 1995; **15**: 5238–5248.
45. Xu W, Ma C, Zhang Q *et al*. PJA1 coordinates with the SMC5/6 complex to restrict DNA viruses and episomal genes in an interferon-independent manner. *J Virol* 2018; **92**: e00825-18.
46. Hebron ML, Lonskaya I, Sharpe K et al. Parkin ubiquitinates Tar-DNA binding protein-43 (TDP-43) and promotes its cytosolic accumulation via interaction with histone deacetylase 6 (HDAC6). *J Biol Chem* 2013; **288**: 4103–4115.
47. Uchida T, Tamaki Y, Ayaki T *et al*. CUL2-mediated clearance of misfolded TDP-43 is paradoxically affected by VHL in oligodendrocytes in ALS. *Sci Rep* 2016; **6**: 19118.
48. Lee YC, Huang WC, Lin JH et al. Znf179 E3 ligase-mediated TDP-43 polyubiquitination is involved in TDP-43- ubiquitinated inclusions (UBI) (+)-related neurodegenerative pathology. *J Biomed Sci* 2018; **25**: 76.
49. Hans F, Fiesel FC, Strong JC *et al*. UBE2E ubiquitin-conjugating enzymes and ubiquitin isopeptidase Y regulate TDP-43 protein ubiquitination. *J Biol Chem* 2014; **289**: 19164–19179.
50. Goldenberg SJ, Marblestone JG, Mattern MR, Nicholson B. Strategies for the identification of ubiquitin ligase inhibitors. *Biochem Soc Trans* 2010; **38**: 132–136.
51. Gabrielsen M, Buetow L, Nakasone MA *et al*. A general strategy for discovery of inhibitors and activators of RING and U-box E3 ligases with ubiquitin variants. *Mol Cell* 2017; **68**: 456–470.